An Efficient Adaptive Distributed Space-Time Coding Scheme for Cooperative Relaying

Jamshid Abouei, Hossien Bagheri, and Amir K. Khandani

Coding and Signal Transmission Laboratory (www.cst.uwaterloo.ca)

Department of Electrical and Computer Engineering, University of Waterloo

Waterloo, Ontario, Canada, N2L 3G1

Tel: 519-884-8552, Fax: 519-888-4338

Emails: {jabouei, hbagheri, khandani}@cst.uwaterloo.ca

Abstract

A non-regenerative dual-hop wireless system based on a distributed space-time coding strategy is considered. It is assumed that each relay retransmits an appropriately scaled space-time coded version of its received signal. The main goal of this paper is to investigate a power allocation strategy in relay stations, which is based on minimizing the outage probability. In the high signal-to-noise ratio regime for the relay-destination link, it is shown that a threshold-based power allocation scheme (i.e., the relay remains silent if its channel gain with the source is less than a prespecified threshold) is optimum. Monte-Carlo simulations show that the derived on-off power allocation scheme performs close to optimum for finite signal-to-noise ratio values. Numerical results demonstrate a dramatic improvement in system performance as compared to the case that the relay stations forward their received signals with full power. In addition, a hybrid amplify-and-forward/detect-and-forward scheme is proposed for the case that the quality of the source-relay link is good. Finally, the robustness of the proposed scheme in the presence of channel estimation errors is numerically evaluated.

Index Terms

Cooperative relaying, space-time coding, outage probability, multi-hop wireless networks.

I. INTRODUCTION

A primary challenge in wireless networks is to mitigate the effect of the multipath fading. Exploiting techniques such as time, frequency and space diversity are the most effective methods to combat the channel fading. Due to the dramatic reduction in the size of wireless devices along with the power and the cost limitations, it is not practical to install multiple antennas on mobile stations. A heuristic solution to this problem is to use a collection of distributed antennas belonging to multiple users [2]–[4]. This new diversity scheme, referred to as cooperative diversity (also known as *cooperative relaying*), has attracted considerable attention in ad hoc and sensor wireless networks in recent years. In particular, this approach is considered as an option in many wireless systems; including IEEE 802.16j mobile multihop relay-based (MMR) networks. Unlike conventional relaying systems that forward the received signal in a relay chain, cooperative relaying takes one step further; i.e., multiple relay nodes work together to achieve a better performance.

Cooperative relay networks have been addressed from different perspectives; including capacity and outage probability analysis [2]–[7], resource allocation (e.g., power allocation [8]), coding [9], relay selection [4], [10], etc. Central to the study of cooperative relay systems is the problem of using *distributed space-time coding* (DSTC) technique as well as efficient power allocation schemes in regenerative and non-regenerative configurations [5], [11]–[18].

The first study on using DSTC scheme in cooperative relay networks was framed in [5] where several relay nodes transmit jointly to the same receiver in order to achieve full spatial diversity in terms of the number of cooperating nodes. Reference [5] analyzes the outage capacity in the high signal-to-noise ratio (SNR) regime. Nabar *et al.* [11] analyze the pairwise error probability of an amplify-and-forward (AF) single-relay system which relies on a DSTC scheme. In [12], the authors investigate the high SNR uncoded bit-error rate (BER) of a two-relay system using

a switching scheme for QPSK modulation. Scutari and Barbarossa [14] analyze the performance of regenerative relay networks with DSTC where the error on the source-relay link propagates into the second phase of the transmission in the relay-destination link. They show how to allocate the transmission power between source and relay to minimize the average BER. The BER of single and dual-hop non-regenerative relay systems with DSTC has been analyzed in [15] where different transmission policies are investigated in order to maximize the end-to-end SNR. The BER of regenerative relay networks using the DSTC scheme, along with different power allocation strategies over non-identical Ricean channels is analyzed in [17]. Zhao *et al.* [8] introduce two power allocation algorithms for AF relay networks to minimize the outage probability without the DSTC scheme.

In this paper, we consider a dual-hop wireless system consisting of a source, two parallel relay stations (RS) and a destination. Assuming that each relay knows its channel with the source, the RSs collaborate with each other by transmitting a space-time coded (STC) version of their received signals to the destination. In such configuration, if the instantaneous received SNR of the relays are unbalanced, the performance of the system degrades substantially. To overcome this problem, an adaptive distributed space-time coding (ADSTC) method is proposed, in which instead of transmitting the noisy signal at each relay with full power, the RS retransmits an appropriately scaled STC version of the received signal. The main goal is to optimize the scaling factor based on the channel-state information (CSI) available at each relay to minimize the outage probability.

The above scheme is different from the power allocation algorithms studied in [8]; primarily we utilize an ADSTC scheme based on the CSI available at each relay, while in [8], no DSTC scheme is used. In our scheme, no information is exchanged between the relay stations. This is to be contrasted with the algorithms proposed in [15], in which the relays need to exchange some information with each other in order to establish which relay transmits. In addition, our scheme is different from the power allocation strategies in [19]–[21], in which the best relays

are selected based on the feedback from the destination.

In the high SNR regime for the relay-destination link, it is shown that a threshold-based power allocation scheme (i.e., the relay remains silent if its channel gain with the source is less than a prespecified threshold) is optimum. Numerical results indicate that the derived on-off power allocation scheme provides a significant performance improvement as compared to the case that the RSs forward their received signals with full power all the time. To further improve the system performance when the quality of the source-relay link is good, a hybrid amplify-and-forward/detect-and-forward scheme is proposed.

In the proposed scheme, we assume that perfect channel knowledge is available at the receiver. In practice, however, the performance of the system is degraded due to the channel estimation error. In the last part of this paper, we address this issue and evaluate the robustness of the proposed scheme in the presence of channel estimation errors.

The rest of the paper is organized as follows. In Section II, the system model and objectives are described. The performance of the system is analyzed in Section III. In Section IV, the simulation results are presented. The effect of channel estimation errors on the proposed scheme is evaluated in Section V. Finally, conclusions are drawn in Section VI.

Notations: Throughout the paper, we use boldface capital and lower case letters to denote vectors and matrices, respectively. $\parallel \mathbf{a} \parallel$ indicates the Euclidean norm of the vector $\mathbf{a}$. The conjugate and conjugated transposition of a complex matrix $\mathbf{A}$ are denoted by $\mathbf{A}^*$ and $\mathbf{A}^\dagger$, respectively. The $n \times n$ identity matrix is denoted by $\mathbf{I}_n$. A circularly symmetric complex Gaussian random variable (r.v.) is represented by $Z = X + jY \sim \mathcal{CN}(0, \sigma^2)$, where X and Y are independent and identically distributed (i.i.d.) normal r.v.'s with $\mathcal{N}(0, \frac{\sigma^2}{2})$. Also, $A \to B$ represents the link from node A to node B. Finally, $\mathbb{P}\{.\}$ and $\mathbb{E}[.]$ denote the probability of the given event and the expectation operator, respectively.

II. System Model and Objectives

In this work, we consider a cooperative relay system consisting of one base station (BS), multiple relay stations randomly located within the network region, and multiple mobile stations (MSs) (Fig. 1-a). All the nodes are assumed to have a single antenna. The relay stations are assumed to be non-regenerative, i.e., they perform some simple operations on the received signals and forward them to the MSs [15]. Also, it is assumed that no information is exchanged between the relays. In this set-up, each pair of the relay stations cooperate with each other to forward their received signals from the source to the destination[1] (Fig. 1-b).

The channel model is assumed to be frequency-flat block Rayleigh fading with the path loss effect. Let us denote the channel coefficients of the links $S \rightarrow RS_i$ and $RS_i \rightarrow D$ as $\mathcal{L}_{sr_i}$ and $\mathcal{L}_{r_i d}$, $i = 1, 2$, respectively. In this case, the channel gain between S and RS_i is represented by $g_{sr_i} \triangleq |\mathcal{L}_{sr_i}|^2 = \Gamma_{sr_i} |h_{sr_i}|^2$, where $\Gamma_{sr_i} \triangleq 10^{-\Upsilon_{sr_i}/10}$ is the gain associated with the path loss Υ_{sr_i} [dB], and the complex random variable h_{sr_i} is the fading channel coefficient. Similarly, the channel gain of the link $RS_i \rightarrow D$ is represented by $g_{r_i d} \triangleq |\mathcal{L}_{r_i d}|^2 = \Gamma_{r_i d} |h_{r_i d}|^2$, where $\Gamma_{r_i d} \triangleq 10^{-\Upsilon_{r_i d}/10}$ and $h_{r_i d}$ are the gain associated with the path loss $\Upsilon_{r_i d}$ [dB] and the channel fading coefficient, respectively. Under the Rayleigh fading channel model, $|h_{sr_i}|^2$ and $|h_{r_i d}|^2$ are exponentially distributed with unit mean (and unit variance). Also, the background noise at each receiver is assumed to be additive white Gaussian noise (AWGN). For this model, communication between S and D is performed based on the following steps: **i) Data Transmission:** This is performed in two phases and through two hops. In the first phase, the source broadcasts the symbols $x[1]$ and $x[2]$ (normalized to have unit energy) to the RSs in two consecutive time slots and over one frequency band. The received discrete-time baseband signal at RS_i is given by

$$u_i[k] = \sqrt{P_s} \mathcal{L}_{sr_i} x[k] + n_{r_i}[k], \quad i = 1, 2, \tag{1}$$

where $k = 1, 2$, represents the transmission time index, P_s is the transmit power of the source

---

[1]In the sequel and for the sake of simplicity of notations, the BS and the MS are denoted by the source (S) and the destination (D), respectively.
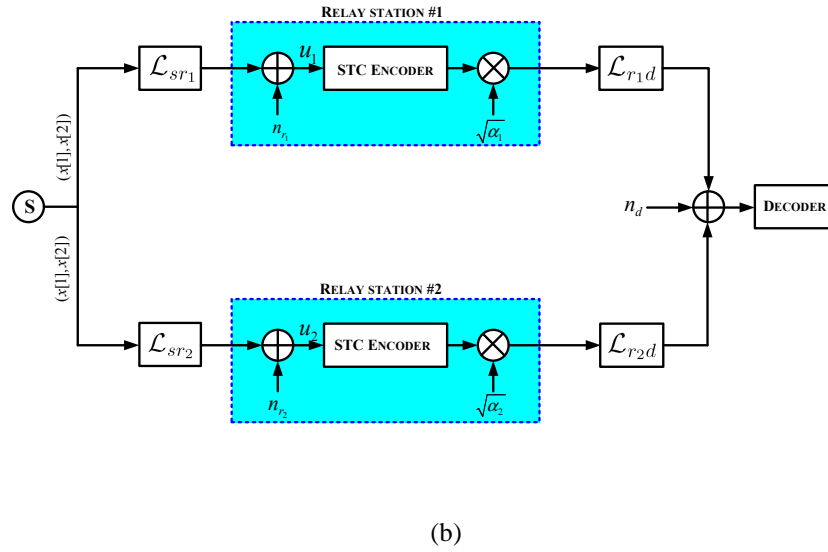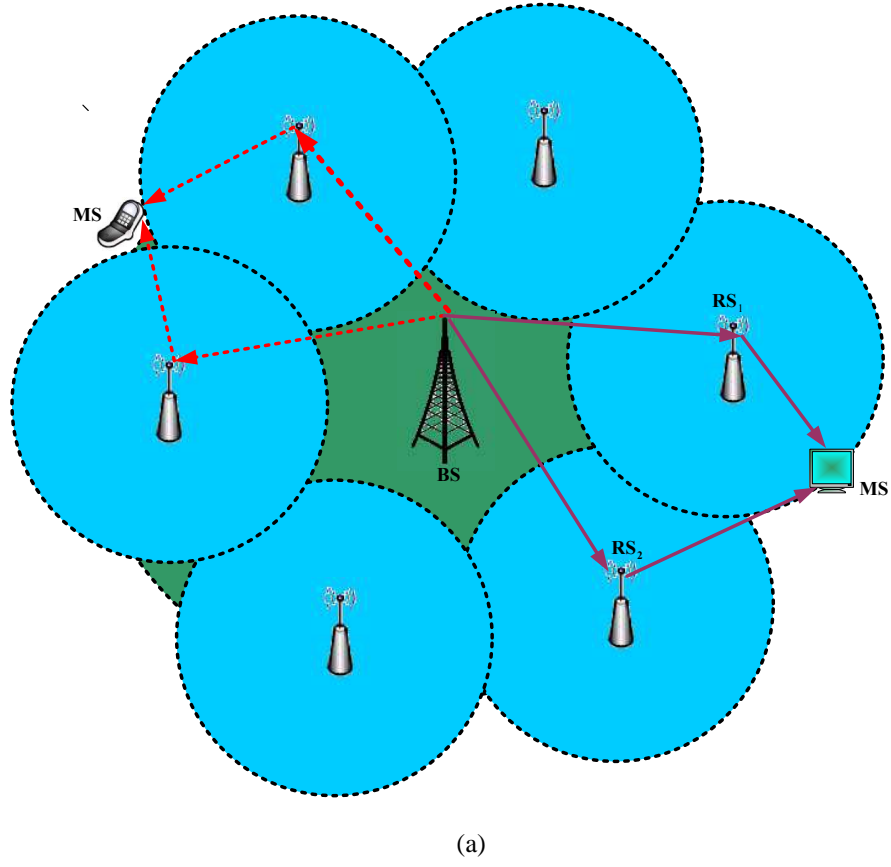
(a)

(b)

Fig. 1.   a) Cooperative relay network, and b) a discrete-time baseband equivalent model of a dual-hop wireless system.

TABLE I

TRANSMISSION POLICY AT RSs

	RS$_1$	RS$_2$
1st time slot	$\sqrt{\alpha_1}e^{-j\theta_{sr_1}}y_1[1]$	$\sqrt{\alpha_2}e^{-j\theta_{sr_2}}y_2[2]$
2nd time slot	$-\sqrt{\alpha_1}\left(e^{-j\theta_{sr_1}}y_1[2]\right)^*$	$\sqrt{\alpha_2}\left(e^{-j\theta_{sr_2}}y_2[1]\right)^*$

and $n_{r_i}[k] \sim \mathcal{CN}(0, N_0)$ is the background noise at RS$_i$. The channel gains are assumed to remain constant over two successive symbol transmissions. Also, we assume that RS$_i$ has perfect information about h_{sr_i}. To satisfy the power constraints at the RSs, we normalize $u_i[k]$ to $\sqrt{\mathbb{E}_x\left[|u_i[k]|^2\Big|h_{sr_i}\right]}$, $i = 1, 2$ [8], [16], [22]. Thus, (1) can be written as

$$y_i[k] = \frac{1}{\sqrt{\mathrm{P}_sg_{sr_i} + N_0}}\left(\sqrt{\mathrm{P}_s}\mathcal{L}_{sr_i}x[k] + n_{r_i}[k]\right), \tag{2}$$

for $i, k = 1, 2$. Using the fact that $x[k]$ is independent of $n_{r_i}[k]$, it yields $\mathbb{E}\left[|y_i[k]|^2\Big|h_{sr_i}\right] = 1$.

In the second phase, the RSs cooperate with each other and forward the space-time coded version of their received noisy signals to the destination over the same or another frequency band[2] (Table I). In such configuration, RS$_i$ multiplies $y_i[.]$ by the scaling factor $\sqrt{\alpha_i}$, where $0 \leq \alpha_i \leq 1$. It should be noted that the phase of S $\rightarrow$ RS$_i$ link, denoted by θ_{sr_i}, is compensated at RS$_i$ through multiplying the received signal by the factor $e^{-j\theta_{sr_i}} = \frac{h_{sr_i}^*}{|h_{sr_i}|}$ [15], [16] [3]. In general, due to the different distances between each RS and D, the arrival time of the received signals at D may be different. The cyclic prefix added to the orthogonal frequency-division multiplexing (OFDM) symbols mitigates the effect of the time delay, and it preserves the orthogonality of the tones. Thus, we can apply the above scheme in each tone.

In each time slot, D receives a superposition of the transmitted signals by RSs. To this end,

[2]It is assumed that RSs use the same transmission protocol based on the IEEE 802.16j time division duplex (TDD) frame structure [23].

[3]We will explain the main reason for using the phase compensation shortly.

the received signals at D in the first and the second time slots are given by

$$r_d[1] = \sqrt{\alpha_1}e^{-j\theta_{sr_1}}y_1[1]\sqrt{P_{r_1}}\mathcal{L}_{r_1d} + \sqrt{\alpha_2}e^{-j\theta_{sr_2}}y_2[2]\sqrt{P_{r_2}}\mathcal{L}_{r_2d} + n_d[1], \tag{3}$$

$$r_d[2] = -\sqrt{\alpha_1}\left(e^{-j\theta_{sr_1}}y_1[2]\right)^*\sqrt{P_{r_1}}\mathcal{L}_{r_1d} + \sqrt{\alpha_2}\left(e^{-j\theta_{sr_2}}y_2[1]\right)^*\sqrt{P_{r_2}}\mathcal{L}_{r_2d} + n_d[2], \tag{4}$$

respectively, where P_{r_i} is the transmit power of RS_i and $n_d[k] \sim \mathcal{CN}(0, N_0)$ represents the background noise at the destination. It should be noted that due to the large distance between S and D (or due to the strong shadowing), we ignore the received signal of the direct link $S \rightarrow D$. Substituting (2) in (3) and (4) yields

$$r_d[1] = \mathcal{L}_1'x[1] + \mathcal{L}_2'x[2] + z_d[1], \tag{5}$$

$$r_d[2] = \mathcal{L}_2'x^*[1] - \mathcal{L}_1'x^*[2] + z_d[2], \tag{6}$$

where

$$\mathcal{L}_i' \triangleq \mathcal{L}_{r_id}\sqrt{\frac{\alpha_i P_s P_{r_i}g_{sr_i}}{P_sg_{sr_i} + N_0}}, \quad i = 1, 2, \tag{7}$$

and

$$z_d[1] \triangleq \frac{\mathcal{L}_1'}{\sqrt{P_s}\mathcal{L}_{sr_1}}n_{r_1}[1] + \frac{\mathcal{L}_2'}{\sqrt{P_s}\mathcal{L}_{sr_2}}n_{r_2}[2] + n_d[1], \tag{8}$$

$$z_d[2] \triangleq -\frac{\mathcal{L}_1'}{\sqrt{P_s}\mathcal{L}_{sr_1}^*}n_{r_1}^*[2] + \frac{\mathcal{L}_2'}{\sqrt{P_s}\mathcal{L}_{sr_2}^*}n_{r_2}^*[1] + n_d[2]. \tag{9}$$

It is observed that $z_d[1]$ is independent of $z_d[2]$ and $\mathbb{E}\left[|z_d[1]|^2\Big|\mathbf{h}\right] = \mathbb{E}\left[|z_d[2]|^2\Big|\mathbf{h}\right] = \sigma^2$, where $\mathbf{h} \triangleq [h_{sr_1}, h_{sr_2}, h_{r_1d}, h_{r_2d}]$ and

$$\sigma^2 \triangleq \left(\frac{|\mathcal{L}_1'|^2}{g_{sr_1}} + \frac{|\mathcal{L}_2'|^2}{g_{sr_2}}\right)\frac{N_0}{P_s} + N_0. \tag{10}$$

ii) Decoding Process: Amplify-and-forward relay networks require full CSI at the destination to coherently decode the received signals. The required channel information can be acquired by transmitting pilot signals[4]. According to the Alamouti scheme [24], we have

$$\begin{bmatrix} r_d[1] \\ r_d^*[2] \end{bmatrix} = \begin{bmatrix} \mathcal{L}_1' & \mathcal{L}_2' \\ \mathcal{L}_2'^* & -\mathcal{L}_1'^* \end{bmatrix}\begin{bmatrix} x[1] \\ x[2] \end{bmatrix} + \begin{bmatrix} z_d[1] \\ z_d^*[2] \end{bmatrix},$$

---

[4] Channel estimation can be done in two steps. In the first step, RS_i transmits a pilot sequence to provide $\mathcal{L}_{r_id}$ to D. In the second step, S transmits another pilot sequence to provide $\mathcal{L}_{sr_i}$ to RS_i and $\mathcal{L}_{sr_i}\mathcal{L}_{r_id}$ to D. In this step, RSs work as usual.

or equivalently $\mathbf{r}_d = \mathcal{L}\mathbf{x} + \mathbf{z}_d$. It is worth mentioning that due to the conjugate terms in (4), the heuristic phase compensation at RSs (i.e., $e^{-j\theta_{sr_i}} = \frac{h_{sr_i}^*}{|h_{sr_i}|}$) is done to preserve the orthogonal property of the processing matrix $\mathcal{L}$, i.e., $\mathcal{L}^\dagger \mathcal{L} = \left(|\mathcal{L}_1'|^2 + |\mathcal{L}_2'|^2\right)\mathbf{I}_2 \triangleq \Lambda\mathbf{I}_2$. Thus, we can use the Alamouti scheme. Also, upon this phase compension assumption and the AF scheme at the relay nodes, the above scenario is converted to the original STC problem. Hence, the mentioned decoder is maximum likelihood (ML) optimal. For this configuration, the input of the ML decoder is given by [25]

$$\tilde{\mathbf{r}}_d \triangleq \mathcal{L}^\dagger \mathbf{r}_d \tag{11}$$

$$= \Lambda\mathbf{x} + \tilde{\mathbf{z}}_d, \tag{12}$$

where $\tilde{\mathbf{z}}_d \triangleq \mathcal{L}^\dagger \mathbf{z}_d$. In this case, the two-dimensional decision rule used in the ML decoder is

$$\hat{\mathbf{x}} = \arg\ \min_{\hat{\mathbf{x}}\in\mathbb{S}^2} \|\tilde{\mathbf{r}}_d - \Lambda\hat{\mathbf{x}}\|^2, \tag{13}$$

where $\mathbb{S}^2$ denotes the corresponding signal constellation set.

Let us denote the average signal-to-noise ratios of $\mathrm{S} \to \mathrm{RS}_i$ and $\mathrm{RS}_i \to \mathrm{D}$ by $\mathrm{SNR}_{sr_i} \triangleq \frac{\mathrm{P}_s}{N_0}\Gamma_{sr_i}$ and $\mathrm{SNR}_{r_id} \triangleq \frac{\mathrm{P}_{r_i}}{N_0}\Gamma_{r_id}$, $i = 1,2$, respectively. Here, we assume that SNR_{sr_i} and SNR_{r_id} are known at RS_i. Assuming h_{sr_i} is available at RS_i, the main objective is to select the optimum factor α_i such that the outage probability is minimized.

III. PERFORMANCE ANALYSIS

In this section, we characterize the performance of the model described in Section II in terms of the outage probability. For this purpose, we first obtain the instantaneous end-to-end SNR. Then, we derive an expression for the outage probability in the high SNR_{r_id} regime.

Since, matrix $\mathcal{L}|\mathbf{h}$ is deterministic and noting that $\mathbb{E}\left[\mathbf{z}_d\mathbf{z}_d^\dagger|\mathbf{h}\right] = \sigma^2\mathbf{I}_2$, we conclude from (12) that

$$\mathbb{E}\left[\tilde{\mathbf{z}}_d\tilde{\mathbf{z}}_d^\dagger|\mathbf{h}\right] = \mathbb{E}\left[\mathcal{L}^\dagger\mathbf{z}_d\mathbf{z}_d^\dagger\mathcal{L}|\mathbf{h}\right] = \Lambda\sigma^2\mathbf{I}_2. \tag{14}$$

In fact, the noise vector $\tilde{\mathbf{z}}_d|\mathbf{h}$ is a white Gaussian noise. Denoting γ as the instantaneous end-to-end SNR and using (12), we have

$$\gamma = \frac{\Lambda^2}{\Lambda\sigma^2} = \frac{|\mathcal{L}_1'|^2 + |\mathcal{L}_2'|^2}{\left(\dfrac{|\mathcal{L}_1'|^2}{g_{sr_1}} + \dfrac{|\mathcal{L}_2'|^2}{g_{sr_2}}\right)\dfrac{N_0}{P_s} + N_0}. \tag{15}$$

In the outage-based transmission framework, the outage occurs whenever γ is less than a threshold $\gamma_t > 0$. In this case, the outage probability can be expressed as

$$P_{out} \triangleq \mathbb{P}\{\gamma < \gamma_t\}. \tag{16}$$

The goal is to minimize the objective function defined in (16) subject to $0 \leq \alpha_i \leq 1$, $i = 1, 2$. The global optimal solution can be obtained through centralized algorithms. This is in contrast to the distributed scheme proposed in Section II. Since, it is difficult to directly compute the exact expression for the outage probability, we first present the outage probability in the high $\text{SNR}_{r_i d}$ regime. Then, we propose an optimum distributed power allocation strategy for the RS_i to minimize the objective function in (16).

Defining $\mathbf{g} \triangleq \left[|h_{sr_1}|^2 = v_1, |h_{sr_2}|^2 = v_2\right]$, and using the fact that the link $\text{S} \to \text{RS}_1$ is independent of the link $\text{S} \to \text{RS}_2$, the outage probability is given by

$$P_{out} = \mathbb{E}_{\mathbf{g}}[\Omega(\mathbf{g})] = \int_0^\infty \int_0^\infty \Omega(\mathbf{g}) e^{-v_1} e^{-v_2} dv_1 dv_2, \tag{17}$$

where $\Omega(\mathbf{g}) \triangleq \mathbb{P}\{\gamma < \gamma_t|\mathbf{g}\}$. It is concluded from (7) and (15) that

$$\Omega(\mathbf{g}) = \mathbb{P}\left\{ \left. \frac{X_1 v_1 + X_2 v_2}{(\dfrac{X_1}{\Gamma_{sr_1}} + \dfrac{X_2}{\Gamma_{sr_2}})\dfrac{N_0}{P_s} + N_0} < \gamma_t \right| \mathbf{g} \right\}, \tag{18}$$

where $X_i \triangleq \mathscr{F}(v_i)|h_{r_i d}|^2$ with

$$\mathscr{F}(v_i) \triangleq \frac{\alpha_i P_s P_{r_i} \Gamma_{sr_i} \Gamma_{r_i d}}{P_s \Gamma_{sr_i} v_i + N_0}, \quad i = 1, 2. \tag{19}$$

Under the Rayleigh fading channel model, $X_i|v_i$ is exponentially distributed with parameter $\frac{1}{\mathscr{F}(v_i)}$ and the probability density function (pdf)

$$f_{X_i|v_i}(x_i|v_i) = \frac{1}{\mathscr{F}(v_i)} e^{-\frac{x_i}{\mathscr{F}(v_i)}} U(x_i), \tag{20}$$

where $U(.)$ is the unit step function. In the high $\text{SNR}_{r_i d}$ regime (i.e., $\text{P}_{r_i}\Gamma_{r_i d} \gg \text{P}_s\Gamma_{sr_i}$ and $\text{P}_{r_i}\Gamma_{r_i d} \gg N_0$, $i = 1, 2$), (18) can be simplified to

$$\Omega(\mathbf{g}) \approx \mathbb{P}\left\{ \left. \frac{X_1 v_1 + X_2 v_2}{(\frac{X_1}{\Gamma_{sr_1}} + \frac{X_2}{\Gamma_{sr_2}})\frac{N_0}{\text{P}_s}} < \gamma_t \right| \mathbf{g} \right\} \tag{21}$$

$$= \mathbb{P}\left\{ \left. \left(v_1 - \frac{\xi}{\Gamma_{sr_1}}\right) X_1 < \left(\frac{\xi}{\Gamma_{sr_2}} - v_2\right) X_2 \right| \mathbf{g} \right\}, \tag{22}$$

where $\xi \triangleq \frac{N_0}{\text{P}_s}\gamma_t$. Depending on the values of v_1 and v_2, we have the following cases:

Case 1: $v_1 < \frac{\xi}{\Gamma_{sr_1}}$ and $v_2 < \frac{\xi}{\Gamma_{sr_2}}$

In this case, (22) can be written as

$$\Omega(\mathbf{g}) = \mathbb{P}\{Z > \phi|\mathbf{g}\} \overset{(a)}{=} 1, \tag{23}$$

where $Z \triangleq \frac{X_1}{X_2}$ and

$$\phi \triangleq \frac{\frac{\xi}{\Gamma_{sr_2}} - v_2}{v_1 - \frac{\xi}{\Gamma_{sr_1}}}. \tag{24}$$

In the above equations, (a) follows from the fact that for $v_1 < \frac{\xi}{\Gamma_{sr_1}}$ and $v_2 < \frac{\xi}{\Gamma_{sr_2}}$, ϕ is negative and this results in $\mathbb{P}\{Z \leq \phi|\mathbf{g}\} = 0$.

Case 2: $v_1 > \frac{\xi}{\Gamma_{sr_1}}$ and $v_2 < \frac{\xi}{\Gamma_{sr_2}}$

From (22), we have

$$\Omega(\mathbf{g}) = \mathbb{P}\left\{Z < \phi|\mathbf{g}\right\}, \tag{25}$$

where ϕ is positive. It can be shown that the pdf of the random variable Z conditioned on the vector $\mathbf{g}$ is obtained as [26]

$$f_{Z|\mathbf{g}}(z|\mathbf{g}) = \frac{\mathscr{F}(v_1)\mathscr{F}(v_2)}{(\mathscr{F}(v_2)z + \mathscr{F}(v_1))^2}U(z). \tag{26}$$

Thus, (25) can be written as

$$\Omega(\mathbf{g}) = \int_0^{\phi} f_{Z|\mathbf{g}}(z|\mathbf{g})dz \tag{27}$$

$$= \frac{\mathscr{F}(v_2)\phi}{\mathscr{F}(v_2)\phi + \mathscr{F}(v_1)}. \tag{28}$$

Case 3: $v_1 < \frac{\xi}{\Gamma_{sr_1}}$ and $v_2 > \frac{\xi}{\Gamma_{sr_2}}$

In this case, (22) can be written as

$$\Omega(\mathbf{g}) \quad = \quad \mathbb{P}\{Z > \phi | \mathbf{g}\} \tag{29}$$

$$= \quad 1 - \mathbb{P}\{Z \le \phi | \mathbf{g}\} \tag{30}$$

$$\stackrel{(a)}{=} \quad \frac{\mathscr{F}(v_1)}{\mathscr{F}(v_2)\phi + \mathscr{F}(v_1)}, \tag{31}$$

where ϕ is positive and (a) comes from (26) and (28).

Case 4: $v_1 > \frac{\xi}{\Gamma_{sr_1}}$ and $v_2 > \frac{\xi}{\Gamma_{sr_2}}$

In this case, since ϕ is negative, we have

$$\Omega(\mathbf{g}) = \mathbb{P}\left\{Z < \phi | \mathbf{g}\right\} = 0. \tag{32}$$

Now, we can use the above results to simplify the outage probability given in (17) for $\mathrm{P}_{r_i}\Gamma_{r_id} \gg \mathrm{P}_s\Gamma_{sr_i}$ and $\mathrm{P}_{r_i}\Gamma_{r_id} \gg N_0$, $i = 1, 2$. Using (23), (28), (31) and (32), we have

$$\mathrm{P}_{out} \quad = \quad \int_0^\infty \int_0^\infty \Omega(\mathbf{g}) e^{-v_1} e^{-v_2} dv_1 dv_2 \tag{33}$$

$$= \quad \int_0^{\frac{\xi}{\Gamma_{sr_1}}} \int_0^{\frac{\xi}{\Gamma_{sr_2}}} 1 e^{-v_1} e^{-v_2} dv_1 dv_2 + \int_0^{\frac{\xi}{\Gamma_{sr_1}}} \left[\int_{\frac{\xi}{\Gamma_{sr_2}}}^\infty \frac{\mathscr{F}(v_1) e^{-v_2}}{\mathscr{F}(v_2)\phi + \mathscr{F}(v_1)} dv_2 \right] e^{-v_1} dv_1$$

$$+ \quad \int_{\frac{\xi}{\Gamma_{sr_1}}}^\infty \left[\int_0^{\frac{\xi}{\Gamma_{sr_2}}} \frac{\mathscr{F}(v_2)\phi e^{-v_2}}{\mathscr{F}(v_2)\phi + \mathscr{F}(v_1)} dv_2 \right] e^{-v_1} dv_1 + \int_{\frac{\xi}{\Gamma_{sr_1}}}^\infty \int_{\frac{\xi}{\Gamma_{sr_2}}}^\infty 0 e^{-v_1} e^{-v_2} dv_1 dv_2 \tag{34}$$

$$= \quad \left(1 - e^{-\frac{\xi}{\Gamma_{sr_1}}}\right)\left(1 - e^{-\frac{\xi}{\Gamma_{sr_2}}}\right) + \int_0^{\frac{\xi}{\Gamma_{sr_1}}} \left[\int_{\frac{\xi}{\Gamma_{sr_2}}}^\infty \frac{e^{-v_2}}{\mathscr{F}(v_2)\phi + \mathscr{F}(v_1)} dv_2 \right] \mathscr{F}(v_1) e^{-v_1} dv_1$$

$$+ \quad \int_0^{\frac{\xi}{\Gamma_{sr_2}}} \left[\int_{\frac{\xi}{\Gamma_{sr_1}}}^\infty \frac{\phi e^{-v_1}}{\mathscr{F}(v_2)\phi + \mathscr{F}(v_1)} dv_1 \right] \mathscr{F}(v_2) e^{-v_2} dv_2. \tag{35}$$

Now, the main objective is to find the optimum scaling factor α_i (or equivalently $\mathscr{F}(v_i)$ defined in (19)) that minimizes the outage probability obtained in (35). Since for $v_1 < \frac{\xi}{\Gamma_{sr_1}}$ and $v_2 > \frac{\xi}{\Gamma_{sr_2}}$, $\phi \triangleq \frac{\frac{\xi}{\Gamma_{sr_2}} - v_2}{v_1 - \frac{\xi}{\Gamma_{sr_1}}} > 0$, it is concluded that the second term in (35) is a nonnegative value. With a similar argument, the third term in (35) is nonnegative as well. Also, we use the fact that $\xi \triangleq \frac{N_0}{\mathrm{P}_s}\gamma_t > 0$. Hence, to minimize (35), it is sufficient to have

$$\int_0^{\frac{\xi}{\Gamma_{sr_1}}} \left[\int_{\frac{\xi}{\Gamma_{sr_2}}}^\infty \frac{e^{-v_2}}{\mathscr{F}(v_2)\phi + \mathscr{F}(v_1)} dv_2 \right] \mathscr{F}(v_1) e^{-v_1} dv_1 \quad = \quad 0, \tag{36}$$

$$\int_0^{\frac{\xi}{\Gamma_{sr_2}}} \left[\int_{\frac{\xi}{\Gamma_{sr_1}}}^\infty \frac{\phi e^{-v_1}}{\mathscr{F}(v_2)\phi + \mathscr{F}(v_1)} dv_1 \right] \mathscr{F}(v_2) e^{-v_2} dv_2 \quad = \quad 0. \tag{37}$$

Noting that $\int_{\frac{\xi}{\Gamma_{sr_2}}}^{\infty} \frac{e^{-v_2}}{\mathscr{F}(v_2)\phi + \mathscr{F}(v_1)} dv_2$ and $\int_{\frac{\xi}{\Gamma_{sr_1}}}^{\infty} \frac{\phi e^{-v_1}}{\mathscr{F}(v_2)\phi + \mathscr{F}(v_1)} dv_1$ are positive, the optimum function $\mathscr{F}(v_i)$ that satisfies (36) and (37) (or equivalently minimizes (35)) is

$$\mathscr{F}(v_i) = 0, \quad \text{for } 0 < v_i < \frac{\xi}{\Gamma_{sr_i}}, \quad i = 1, 2 \tag{38}$$

In this case,

$$\min \mathrm{P}_{out} = \left(1 - e^{-\frac{\xi}{\Gamma_{sr_1}}}\right)\left(1 - e^{-\frac{\xi}{\Gamma_{sr_2}}}\right) \tag{39}$$

$$\overset{(a)}{=} \left(1 - e^{-\frac{\gamma_t}{\mathrm{SNR}_{sr_1}}}\right)\left(1 - e^{-\frac{\gamma_t}{\mathrm{SNR}_{sr_2}}}\right), \tag{40}$$

where (a) comes from $\xi \triangleq \frac{N_0}{P_s}\gamma_t$ and $\mathrm{SNR}_{sr_i} \triangleq \frac{P_s}{N_0}\Gamma_{sr_i}$. Using (19) and (38), we come up with the following result:

$$\hat{\alpha}_i = 0, \quad 0 < g_{sr_i} < \xi, \quad i = 1, 2, \tag{41}$$

where $\hat{\alpha}_i$ is the optimum scaling factor that minimizes the outage probability. In other words, the relay remains silent if its channel gain with the source is less than the threshold level ξ. Note that we are not concerned with the computation of the exact values of the scaling factors at the relay nodes, i.e., $\hat{\alpha}_i$ for $v_i \geq \frac{\xi}{\Gamma_{sr_i}}$, as long as $P_{r_i}\Gamma_{r_id} \gg P_s\Gamma_{sr_i}$ and $P_{r_i}\Gamma_{r_id} \gg N_0$, $i = 1, 2$.

Remark 1- The case of high SNR_{sr_i} is similar to the traditional STC problem. Therefore, the optimum power allocation policy for relay stations is the full power transmission.

IV. NUMERICAL RESULTS

In this section, we present some Monte-Carlo simulation results to evaluate the impact of α_i on the system performance. We use the propagation model with *intermediate path-loss condition* (i.e., terrain type B for suburban, above roof top (ART) to below roof top (BRT)) provided by WiMAX Forum and IEEE 802.16j relay Working Group (WG) [27], i.e.,

$$\Upsilon_{ij} \triangleq \begin{cases} 20\log_{10}\left(\frac{4\pi d_{ij}}{\lambda}\right), & d_{ij} \leq d_0' \\ K + 10\beta\log_{10}\left(\frac{d_{ij}}{d_0}\right) + \Delta\Upsilon_f + \Delta\Upsilon_{h_t}, & d_{ij} > d_0', \end{cases}$$

where $\Upsilon_{ij} \triangleq -10\log_{10}\Gamma_{ij}$ is the path loss between nodes i and j expressed in dB, and

- d_{ij} is the distance between nodes i and j,

TABLE II

Parameters	Values
Carrier frequency	2.4 GHz
$\text{SNR}_{r_i d}$, $i = 1, 2$	$0 - 40$ dB
d_0	100 m
Antenna height	BS=32 m, RS=15 m, MS=1.5 m
Distance between S and RS	$d_{sr_1} = 5$ km, $d_{sr_2} = 8$ km
Distance between RS and D	$d_{r_1 d} = 2$ km, $d_{r_2 d} = 1$ km
Path loss exponent parameters	$a = 4$, $b = 0.0065$, $c = 17.1$

- λ is the wavelength,

- β is the path loss exponent,

- d_0 is the reference distance,

- $d_0' \triangleq d_0 10^{-\frac{\Delta\Upsilon_f + \Delta\Upsilon_{h_t}}{10\beta}}$

- $\Delta\Upsilon_f$ is the correction factor for the carrier frequency f,

- $\Delta\Upsilon_{h_t}$ is the correction factor for the RS/MS BRT antenna height h_t,

- $K \triangleq 20\log_{10}\left(\frac{4\pi d_0'}{\lambda}\right)$.

For this model, β, $\Delta\Upsilon_f$ and $\Delta\Upsilon_{h_t}$ are given as [27]

$$\beta \triangleq a - bh_b + \frac{c}{h_b},$$

$$\Delta\Upsilon_f \triangleq 6\log_{10}\left(\frac{f(\text{MHz})}{2000}\right),$$

$$\Delta\Upsilon_{h_t} \triangleq \begin{cases} -10\log_{10}\left(\frac{h_t}{3}\right), & h_t \leq 3 \text{ m} \\ -20\log_{10}\left(\frac{h_t}{3}\right), & h_t > 3 \text{ m}, \end{cases}$$

respectively, where h_b represents the height of BS/RS ART antenna. Using the system parameters listed in Table II, the desired SNR_{sr_i} and $\text{SNR}_{r_i d}$ are obtained through adjusting $\frac{P_s}{N_0}$ and $\frac{P_{r_i}}{N_0}$, respectively.

We consider some forms of the scaling factors α_i in terms of g_{sr_i}. In the *full power* scheme, each relay retransmits its received signal with full power (i.e., $\alpha_i = 1$), regardless of the value of g_{sr_i}. For the *on-off power* scheme, RS_i with g_{sr_i} above certain threshold transmits at full power, otherwise it remains silent, i.e., $\alpha_i = 0$. We also consider the *piecewise linear function* scheme, in which the scaling factor α_i is defined as

$$\alpha_i \triangleq \begin{cases} 0, & g_{sr_i} < \tau_1 \\ \dfrac{1}{\tau_2 - \tau_1} g_{sr_i} - \dfrac{\tau_1}{\tau_2 - \tau_1}, & \tau_1 \leq g_{sr_i} < \tau_2 \\ 1, & g_{sr_i} \geq \tau_2, \end{cases} \tag{42}$$

where the optimum values of τ_1 and τ_2 are obtained using an exhaustive search to minimize the outage probability. This function can approximate a large class of appropriate functions[5] by adjusting τ_1 and τ_2. In addition, we use the ML decoder at D to fully exploit the diversity advantage of the proposed scheme.

Fig. 2 compares the outage probability of the aforementioned power schemes versus γ_t for different values of $\text{SNR}_{r_1 d} = \text{SNR}_{r_2 d} \triangleq \text{SNR}_{rd}$. The results are obtained by averaging over 10^6 channel realizations. We can observe a significant performance improvement for the on-off power scheme in comparison with the full power scenario, as SNR_{rd} increases. For instance, 10 dB gain is obtained using the on-off power strategy for $\text{SNR}_{rd} = 40$ dB and $P_{out} = 10^{-2}$ with respect to the full power scheme. Also, it can be seen that the optimized piecewise linear function performs close to the on-off scheme. Table III shows the optimum threshold level of the on-off power scheme expressed in dB for different values of γ_t and SNR_{rd}, and $\text{SNR}_{sr_1} = \text{SNR}_{sr_2} = 25$ dB. It is interesting to note that the optimum threshold values obtained by exhaustive search are close to ξ (dB) $= \gamma_t$ (dB) $- \text{SNR}_{sr_i}$ (dB) obtained in Section III.

In Fig. 3, we plot the outage probabilities of the centralized scheme, iterative algorithm and the on-off power allocation strategy with the threshold ξ obtained in Section III. In the centralized approach, the optimum α_1 and α_2 are obtained through an exhaustive search to minimize the

---

[5]The optimum function should have small values when the channel is weak and should increase up to 1 as the channel gain increases.
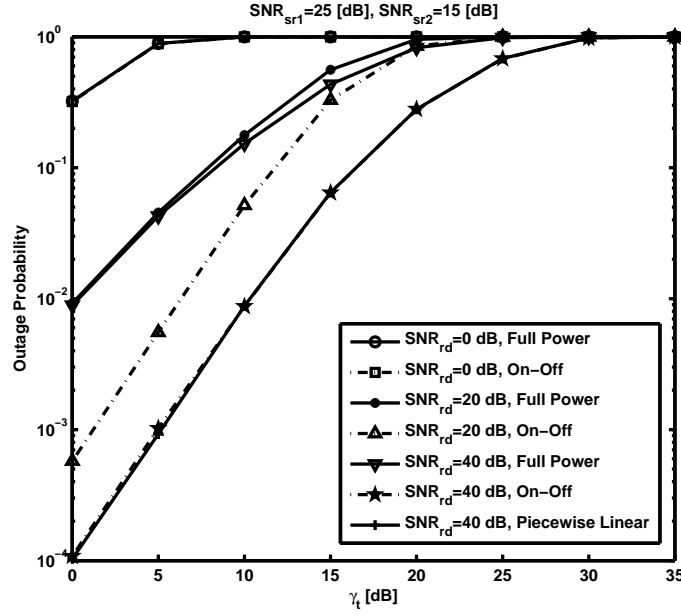
Fig. 2. Outage probability versus γ_t for different strategies.

TABLE III

OPTIMUM THRESHOLD LEVEL FOR THE ON-OFF POWER SCHEME

	$\text{SNR}_{rd} = 0$ dB	$\text{SNR}_{rd} = 10$ dB	$\text{SNR}_{rd} = 20$ dB	$\text{SNR}_{rd} = 30$ dB	$\text{SNR}_{rd} = 40$ dB
$\gamma_t = 0$ dB	-25	-25	-25	-25	-25
$\gamma_t = 10$ dB	-13	-15	-15	-15	-15
$\gamma_t = 20$ dB	0	-1.5	-5	-5	-5
$\gamma_t = 30$ dB	0	0	0	0	0

outage probability. In the iterative scheme, the algorithm starts from an initial value of α_1 for every g_{sr_i}. Then, for each value of g_{sr2}, α_2 is obtained such that the outage probability is minimized. This process continues until the algorithm converges. The results in Fig. 3 show that the difference in performance between the proposed on-off power scheme and the centralized approach is small. Therefore, the on-off scheme obtained by the asymptotic analysis in Section III is almost optimal.

Fig. 4 plots the uncoded BER versus SNR_{rd} for different power schemes and BPSK constellation. We observe an error floor in the figure for the high SNR_{rd}. This can be attributed to the amplified noise received at the destination through the $R \rightarrow D$ link. In this case, the performance
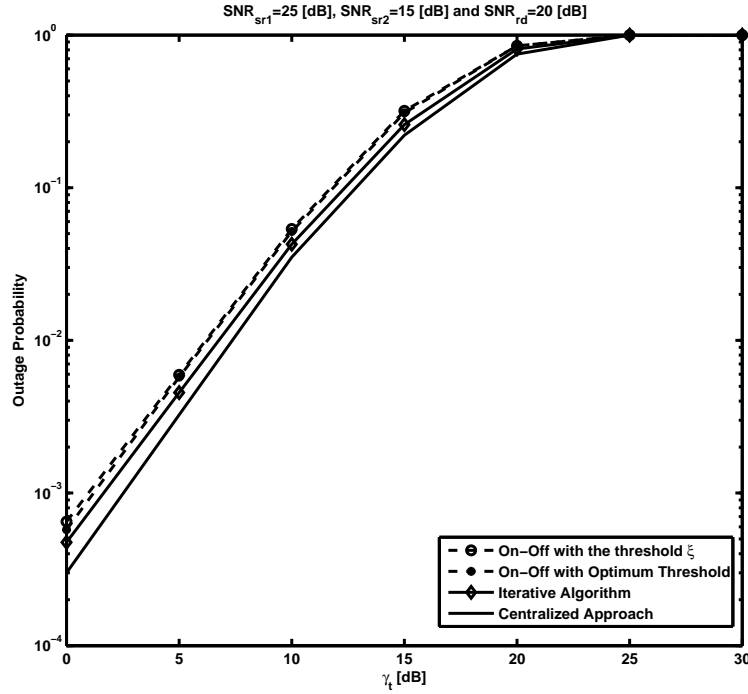
Fig. 3. Outage probability versus γ_t for different power schemes.

is governed by SNR_{sr_i}, $i = 1, 2$.

It should be noted that by using the on-off power allocation strategy at RSs, we can save the energy in the silent mode. However, simulation results implies that the power saving gain in the on-off power scheme is negligible. This is due to the fact that for mid-SNR_{sr_i} region, $P_{ON} \triangleq \Pr\{g_{sr_i} > g_{Th}\} \geq 0.95$, where g_{Th} is the optimum threshold level that minimizes the BER.

Fig. 5-a illustrates the frame-error rate (FER) versus $(E_b/N_0)_{rd}$, energy per bit to noise density ratio, using the standard turbo code [28] with the rate of $1/3$ and for different functions of α_i, BPSK constellation and the frame length of 957 bits. Also, Fig. 5-b illustrates the FER versus $(E_b/N_0)_{rd}$ using the convolutional code (introduced in section $8.4.9.2.1$ of the IEEE 802.16e standard [29]) with the rate of 0.5 and the frame length of 576 bits. Compared to the full power scheme, the simulation results show a significant improvement in the system performance with the on-off power scheme. Also, it is observed from the simulation that the trend of the FER for
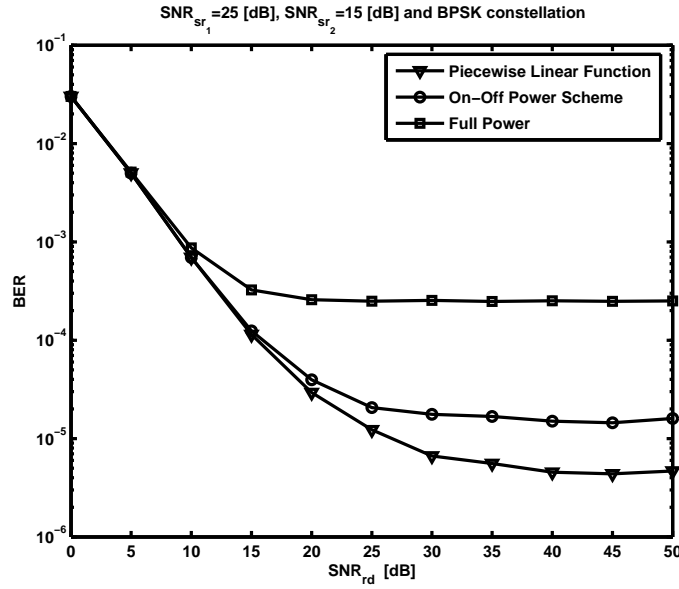
Fig. 4.   Uncoded BER versus SNR_{rd} for different power schemes.

higher order constellations is similar to the BPSK case [26].

Up to now, we have shown that the near-optimal power allocation in each relay in the AF mode is the threshold-based on-off power scheme. To further improve the system performance when the quality of S→RS_i is good, the detect-and-forward (DF) scheme is suggested to eliminate the amplified noise at the RS. A *hybrid threshold-based AF/DF* scheme characterized by two threshold levels T_1 and T_2 is described as follows:

1- For $g_{sr_i} \leq T_2$, RS_i performs the on-off power scheme developed in Section III.

2- For $g_{sr_i} > T_2$, RS_i detects $x[k]$, $k \in \{1, 2\}$, from the received signal and forwards the detected symbol $\hat{x}[k]$ to the destination.

Fig. 6 compares the FER of different transmission strategies in the RSs for the convolutional code with QPSK modulation and the frame length of 576 bits. In the pure full power scheme, independent of the channel gain g_{sr_i}, each RS_i transmits with full power all the time. For completeness, we also consider the threshold-based DF scheme, in which for g_{sr_i} less than a prescribed threshold, RS_i remains silent, otherwise it switches to the DF mode. It is observed that the performance of the hybrid threshold-based AF/DF scheme is the same as the threshold-
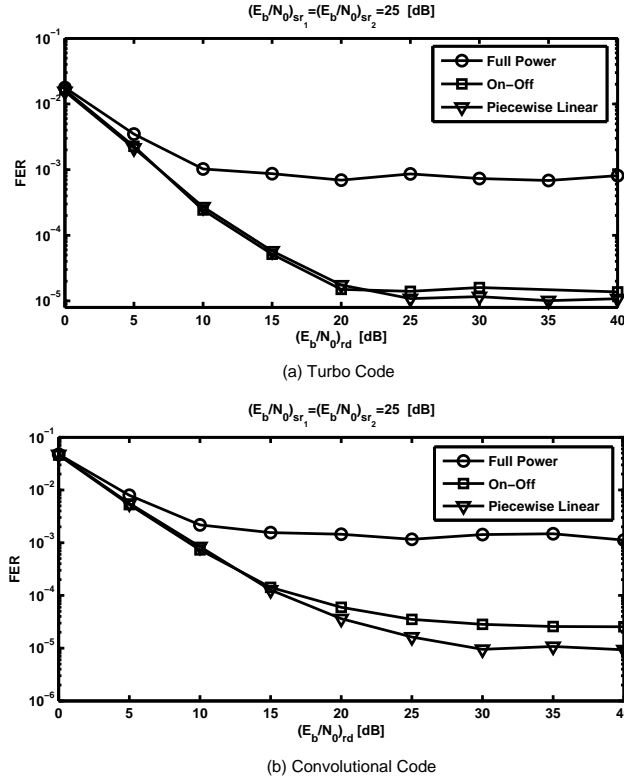
Fig. 5.   FER versus $(E_b/N_0)_{rd}$ for different power schemes and for a) turbo code with the rate $1/3$ b) convolutional code with the rate $1/2$.

based AF on-off power scheme and both of them are better than the pure full power and the threshold-based DF schemes.

V. IMPACT OF CHANNEL ESTIMATION ERROR

Throughout this paper, it is assumed that perfect channel knowledge is available at the receiver. In practice, however, the channel estimation at the receiver is often imperfect. Thus, the performance of the system is degraded due to the channel estimation error[6]. In this section, we evaluate the FER degradation of the proposed scheme due to the imperfect channel estimation. To handle that, a pilot-based channel estimation technique is assumed, where pilot sequences are inserted at the beginning of each block. It is assumed that the pilot sequences have the same energy as data symbols. In this case, the channel estimation process is performed at the beginning

[6]Such a problem has been first studied by Alamouti [24] and Tarokh [30] in STC-based systems. This line of work is further extended for different structures of the receiver (See [31] and its references).
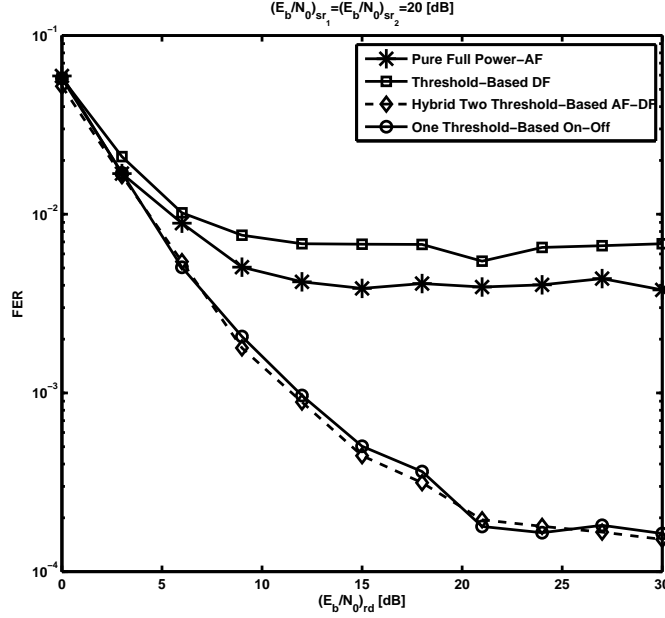
Fig. 6. FER versus $(E_b/N_0)_{rd}$ for different transmission strategies and for convolutional code with the rate $1/2$, $(E_b/N_0)_{sr} =$ 20 dB and for QPSK.

of each block and the estimated value remains constant over the block. This assumption is valid under the frequency-flat Rayleigh fading channel model, where the multipath channel coefficients change slowly and are considered constant. Due to the imperfect channel estimation, the channel fading coefficients can be expressed as

$$\hat{h}_{sr_i} = h_{sr_i} + e_{sr_i}, \tag{43}$$

$$\hat{h}_{r_i d} = h_{r_i d} + e_{r_i d}, \tag{44}$$

for $i = 1, 2$, where e_{sr_i} and $e_{r_i d}$ represent the channel estimation errors which are modeled as independent complex Gaussian random variables with zero means and variances ϑ_{sr_i} and $\vartheta_{r_i d}$, respectively. We assume that the channel estimation error has the variance equal to the inverse of the signal-to-noise ratio of the corresponding link [30], [32], [33], i.e., $\vartheta_{sr_i} = 1/\text{SNR}_{sr_i}$ and $\vartheta_{r_i d} = 1/\text{SNR}_{r_i d}$.

Fig. 7 shows the FER performance of the full power and the on-off power schemes versus SNR_{rd} for perfect and imperfect CSI situations. We observe that for the low SNR_{rd}, the robustness of the on-off power scheme is close to the full power case. However, for high SNR_{rd} regime,
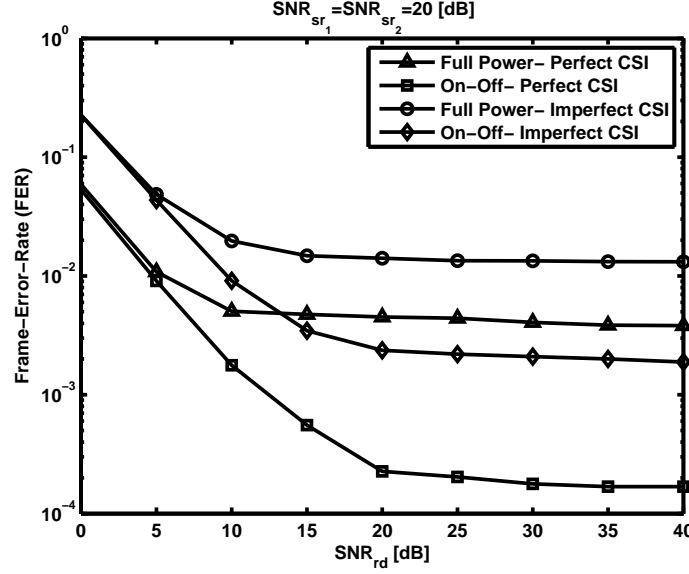
Fig. 7. FER versus SNR_{rd} for the full power and the on-off power allocation schemes for perfect and imperfect CSI.

the full power scheme is more robust to channel estimation errors than the on-off power scheme. This is due to the fact that in the on-off scheme, each relay i requires CSI of the link $\mathrm{S} \to \mathrm{RS}_i$ for scaling factor computation. It is obvious that in this case, imperfect CSI further deteriorates the performance. Note that at low SNR_{rd}, the performance is governed by the second link. In this case, CSI of the link $\mathrm{RS}_i \to \mathrm{D}$ becomes equally important in both schemes.

VI. CONCLUSION

In this paper, a non-regenerative dual-hop wireless system based on a distributed space-time coding strategy is considered. It is assumed that each relay forwards an appropriately scaled space-time coded version of its received signal. In the high $\mathrm{SNR}_{r_i d}$, it has been shown that the optimum power allocation strategy in each RS_i which minimizes the outage probability is to remain silent, if g_{sr_i} is less than a prespecified threshold level. Simulation results show that the threshold-based on-off power scheme performs close to optimum for finite SNR values. Numerical results demonstrate a dramatic improvement in system performance as compared to the case that the relay stations forward their received signals with full power. The practical advantage of using this protocol is that it does not alter the Alamouti decoder at the destination,

while it slightly modifies the relay operation.

ACKNOWLEDGMENT

REFERENCES

[1] J. Abouei, H. Bagheri, and A. K. Khandani, "An efficient adaptive distributed space time coding scheme for cooperative relaying," in *Proc. IEEE 42nd Conference of Information Sciences and Systems (CISS'08)*, Princeton University, Princeton, NJ, USA, March 2008.

[2] A. Sendonaris, E. Erkip, and B. Aazhang, "User cooperation diversity: Part I system description," *IEEE Trans. on Commun.*, vol. 51, no. 11, pp. 1927–1938, Nov. 2003.

[3] A. Sendonaris, E. Erkip, and B. Aazhang, "User cooperation diversity: Part II implementation aspects and performance analysis," *IEEE Trans. on Commun.*, vol. 51, no. 11, pp. 1939–1948, Nov. 2003.

[4] J. N. Laneman, D. N. C. Tse, and G. W. Wornell, "Cooperative diversity in wireless networks: Efficient protocols and outage behavior," *IEEE Trans. on Inform. Theory*, vol. 50, no. 12, pp. 3062–3080, Dec. 2004.

[5] J. N. Laneman and G. W. Wornell, "Distributed space-time coded protocols for exploiting cooperative diversity in wireless networks," *IEEE Trans. on Inform. Theory*, vol. 49, pp. 2415–2425, Sept. 2003.

[6] M. O. Hasna and M. S. Alouini, "A performance study of dual-hop transmissions with fixed gain relays," *IEEE Trans. on Wireless Commun.*, vol. 3, no. 6, pp. 1963–1968, Nov. 2004.

[7] A. H. Madsen and J. Zhang, "Capacity bounds and power allocation for the wireless relay channel," *IEEE Trans. on Inform. Theory*, vol. 51, no. 6, pp. 2020–2040, June 2005.

[8] Y. Zhao, R. Adve, and T. J. Lim, "Improving amplify-and-forward relay networks: optimal power allocation versus selection," *IEEE Trans. on Wireless Commun.*, vol. 6, no. 8, pp. 3114–3123, August 2007.

[9] G. Kramer, M. Gastpar, and P. Gupta, "Cooperative strategies and capacity theorems for relay networks," *IEEE Trans. on Inform. Theory*, vol. 51, no. 9, pp. 3037–3063, Sept. 2005.

[10] A. Bletsas, A. Khisti, D. P. Reed, and A. Lippman, "A simple cooperative diversity method based on network path selection," *IEEE Journal on Selected Areas of Commun.*, vol. 24, no. 3, pp. 659–672, March 2006.

[11] R. U. Nabar, H. Bolcskei, and F. W. Kneubuhler, "Fading relay channels: performance limits and space-time signal design," *IEEE Journal on Selected Areas in Commun.*, vol. 22, no. 6, pp. 1099–1109, August 2004.

[12] Y. Chang and Y. Hua, "Diversity analysis of orthogonal space-time modulation for distributed wireless relays," in *Proc. Int. Conf. on Acoustics, Speech, and Signal Proc.*, May 2004, vol. 4, pp. 561–564.

[13] T. Miyano, H. Murata, and M. Araki, "Space time coded cooperative relaying technique for multihop communications," in *Proc. IEEE Vehicular Technology Conference*, Fall 2004, vol. 7, pp. 5140–5144.

[14] G. Scutari and S. Barbarossa, "Distributed space-time coding for regenerative relay networks," *IEEE Trans. on Wireless Communin.*, vol. 4, no. 5, pp. 2387–2399, Sept. 2005.

[15] P. A. Anghel and M. Kaveh, "On the performance of distributed space-time coding systems with one and two non-regenerative relays," *IEEE Trans. on Wireless Commun.*, vol. 5, no. 3, pp. 682–692, March 2006.

[16] H. Rong, Z. Zhang, and P. Larsson, "Cooperative relaying based on Alamouti diversity under aggregate relay power constraints," in *Proc. IEEE VTC'06 Conference*, Spring 2006, vol. 5, pp. 2563–2567.

[17] J. He and P. Y. Kam, "On the performance of distributed space-time block coding over nonidentical ricean channels and the optimum power allocation," in *Proc. IEEE ICC '07*, June 2007, pp. 5592–5597.

[18] X. Guo and X.-G. Xia, "A distributed space-time coding in asynchronous wireless relay networks," *IEEE Trans. on Wireless Commun.*, vol. 7, no. 5, pp. 1812–1816, May 2008.

[19] L. Zhang and L. J. Cimini Jr., "Power-efficient relay selection in cooperative networks using decentralized distributed space-time block coding," *EURASIP Journal on Advances in Signal Processing*, 2008.

[20] M. Chen, S. Serbetli, and A. Yener, "Distributed power allocation for parallel relay networks," in *Proc. IEEE Globecom Conference*, 2005, pp. 1177–1181.

[21] C. K. Lo, R. W. Heath Jr., and S. Vishwanath, "Opportunistic relay selection with limited feedback," in *Proc. IEEE VTC'07*, Fall 2007, pp. 135–139.

[22] A. Ribeiro, X. Cai, and G. B. Giannakis, "Symbol error probabilities for general cooperative links," *IEEE Trans. on Wireless Communin.*, vol. 4, no. 3, pp. 1264–1273, May 2005.

[23] IEEE 802.16j-06/026r4, "Part 16: Air interface for fixed and mobile broadband wireless access systems, Multihop relay specification," in *IEEE 802.16j WG*, June 2007.

[24] S. M. Alamouti, "A simple transmit diversity technique for wireless communications," *IEEE Journal on Selected Areas in Commun.*, vol. 16, no. 8, pp. 1451–1458, Oct. 1998.

[25] V. Tarokh, H. Jafarkhani, and A. R. Calderbank, "Space-time block codes from orthogonal designs," *IEEE Trans. on Inform. Theory*, vol. 45, no. 5, pp. 1456–1467, July 1999.

[26] J. Abouei, H. Bagheri, and A. K. Khandani, "A new adaptive distributed space-time-coding scheme for cooperative relaying," Technical report, UW-ECE #2007-37, University of Waterloo, ECE Dept., Nov. 2007, available at http://www.cst.uwaterloo.ca/pubtech-rep.html.

[27] IEEE 802.16j-06/013r3, "Multi-hop relay system evaluation methodology (channel model and performance metric)," in *IEEE 802.16j WG*, Feb. 2007.

[28] C. Berrou, A. Glavieux, and P. Thitimajshima, "Near Shannon limit error-correcting coding and decoding: Turbo-codes," in *Proc. ICC'93*, May 1993, vol. 2, pp. 1064–1070.

[29] IEEE Standards, "Part 16: Air interface for fixed and mobile broadband wireless access systems," in *IEEE802.16e Standards*, 2005.

[30] V. Tarokh, A. Naguib, N. Seshadri, and A. R. Calderbank, "Space-time codes for high data rate wireless communication:

performance criteria in the presence of channel estimation errors, mobility, and multiple paths," *IEEE Trans. on Communications*, vol. 47, no. 2, pp. 199–207, Feb. 1999.

[31] W. Hoteit, Y. R. Shayan, and A. K. Elhakeem, "Effects of imperfect channel estimation on space-time coding performance," *IEE Proc.-Commun.*, vol. 152, no. 3, pp. 277–281, June 2005.

[32] R. M. Buehrer and N. A. Kumar, "The impact of channel estimation error on space-time block codes," in *Proc. IEEE 56th Vehicular Technology Conference*, Sept. 2002, vol. 3, pp. 1921–1925.

[33] D. Mavares and R. P. Torres, "Channel estimation error effects on the performance of STB codes in flat frequency Rayleigh channels," in *Proc. IEEE 58th Vehicular Technology Conference*, Oct. 2003, vol. 1, pp. 647–651.